Electronic Supplementary Material (ESI) for ChemComm.

Supporting Information

Improved single-chain-magnet behavior in a biradical-based nitronyl nitroxide-Cu-Dy chain

Jing Xie,[a] Hong-Dao Li,[a] Meng Yang,[a] Juan Sun,[a] Li-Cun Li,*[a] and Jean-Pascal Sutter*[b]

[a.] *Department of Chemistry, Key Laboratory of Advanced Energy Materials Chemistry, College of Chemistry, Nankai University, Tianjin 300071, China*

E-mail: llicun@nankai.edu.cn.

[b.] *LCC-CNRS, Université de Toulouse, Toulouse, France*

E-mail: sutter@lcc-toulouse.fr.

Experimental section

Experimental section

1. Materials and Physical Measurements

All reagents and solvents were purchased from commercial sources and used as received. The biradical ligand bisNITPhPy was prepared according to literature method.[S1] Elemental analysis (for C, H, and N) was implemented on a PerkinElmer 240 elemental analyzer. Infrared spectra were measured in the 4000–400 cm^{-1} range on KBr pellets using a Bruker TENOR 27 spectrometer. Magnetic measurements were performed on a Quantum Design MPMS 5 SQUID magnetometer using crystalline powder samples mixed to grease. Magnetic susceptibility data were corrected for the diamagnetic contribution of all the constituent atoms with Pascal's constants and the sample holder.

2. Synthesis

$[DyCu_2(hfac)_7(bisNITPhPy)]$ 1

A mixture of $Dy(hfac)_3 \cdot 2H_2O$ (0.01 mmol,0.0082g) and $Cu(hfac)_2$ (0.02 mmol, 0.009 g) was dissolved in 15 mL dry boiling *n*-hexane. The solution was maintained to reflux for 6 h, then cooled to 50 ℃ and bisNITPhPy ligand (0.01 mmol, 0.0047 g) in a $CHCl_3$ solution (6 mL) was added to the above solution. The resulting solution was heated for 15 min and then was cooled to room temperature, filtered, and stored at room temperature for slow evaporation. After a week, dark-green strip crystals were obtained for single crystal X-ray analysis. Yield: 65%. Calcd for $C_{60}H_{38}Cu_2F_{42}DyN_5O_{18}$ (2204.56 g mol^{-1}): C, 32.69; H, 1.72; N, 3.18. Found: C, 32.67; H, 2.05; N, 3.25. FT-IR (KBr): 3417(m)，2877(m), 2432(m), 1789(m), 1653(s), 1533(s), 1477(s), 1360(s) , 1154(s), 1074(s), 949(s), 860(s), 662(s), 588(m), 547(s) cm^{-1}.

3. X-ray crystallography

The crystal data were collected at 113 K on a Rigaku Saturn CCD diffractometer (Mo/Kα radiation, λ = 0.71073 Å). The multi-scan absorption corrections were conducted using the SADABS program.[S2] These structures were solved by direct methods and then refined by full-matrix least-squares on F^2 using crystallographic software package program SHELXS-2014.[S3] Non-H atoms were refined anisotropically. All hydrogen atoms were set in calculated positions and refined as riding on the corresponding non-hydrogen atoms. Information concerning detailed crystallographic data collections and structure refinements parameters are provided in Table S1. Selected bond distances (Å) and angles (°) are shown in Table S2. Crystallographic data for the structural analyses have been deposited with the Cambridge Crystallographic Data Centre, CCDC 1879743 contain the supplementary crystallographic data for complex **1.** These information can be obtained free of charge via www.ccdc.cam.ac.uk/data_request/cif.

Table S1 Crystallographic data and structure refinement parameters for **1**.

Complex	**1Dy**
Empirical formula	$C_{60}H_{38}Cu_2F_{42}DyN_5O_{18}$
Mr	2204.53
T (K)	113
Crystal system	monoclinic
Space group	$P2_1/c$
a/Å	20.944(4)
b/Å	20.520(4)
c/Å	19.008(4)
α/ °	90.000
β/ °	95.45(3)
γ/ °	90.000
V/Å^3	8132(3)
Z	4
D_{calcd}/g cm^{-3}	1.801
μ/mm^{-1}	1.590
θ/ °	1.816to 25.009
F(000)	4316
Collected reflections	64162
Independent reflections	14313
R_{int}	0.0749
GOF(F^2)	1.069
R1/wR2 ($I > 2\sigma(I)$)	0.0806/0.2053
R1/wR2 (all data)	0.0997/0.2218

Table S2 Selected bond lengths [Å] and angles [°] for **1.**

Bond distance			
Dy(1)-O(2)	2.367(5)	Cu(2)-O(1)	2.388(6)
Dy (1)-O(3)	2.385(5)	Cu(2)-O(1)#1	2.388(6)
Dy (1)-O(13)	2.347(6)	Cu(2)-O(9)	1.932(6)
Dy (1)-O(14)	2.368(6)	Cu(2)-O(10)	1.938(6)
Dy (1)-O(15)	2.298(5)	Cu(3)-O(4)	2.604(6)
Dy (1)-O(16)	2.374(5)	Cu(3)-O(4)#1	2.604(6)
Dy (1)-O(17)	2.306(6)	Cu(3)-O(11)	1.939(6)
Dy (1)-O(18)	2.374(5)	Cu(3)-O(12)	1.922(6)
Cu(1)-N(1)	2.038(7)	O(1)-N(2)	1.259(9)
Cu(1)-O(5)	1.995(7)	O(2)-N(3)	1.304(8)
Cu(1)-O(6)	1.935(6)	O(3)-N(4)	1.293(8)
Cu(1)-O(7)	2.129(6)	O(4)-N(5)	1.268(9)
Cu(1)-O(8)	1.943(6)		
Angle			
O(2)-Dy(1)-O(3)	82.4(7)	O(1)-Cu(2)-O(1)#1	180.0
O(13)-Dy(1)-O(2)	115.9(2)	O(9)#1-Cu(2)-O(9)	180.0
O(13)-Dy(1)-O(3)	71.3(1)	O(10)#1-Cu(2)-O(10)	180.0
O(15)-Dy(1)-O(2)	146.3(2)	O(10)-Cu(2)-O(1)	98.3(3)
O(15)-Dy(1)-O(3)	83.6(2)	O(10)-Cu(2)-O(1)#1	81.7(3)
O(17)-Dy(1)-O(2)	84.0(2)	O(4)-Cu(3)-O(4)#1	180.0
O(17)-Dy(1)-O(3)	142.8(3)	O(11)-Cu(3)-O(11)#2	180.0
O(5)-Cu(1)-O(6)	90.9(3)	O(12)-Cu(3)-O(12)#2	180.0
O(7)-Cu(1)-O(8)	89.7(2)	N(3)-O(2)-Dy(1)	136.6(5)
O(5)-Cu(1)-N(1)	144.2(3)	N(4)-O(3)-Dy(1)	138.7(4)
O(6)-Cu(1)-N(1)	93.1(3)	N(2)-O(1)-Cu(2)	147.3(7)
O(7)-Cu(1)-N(1)	108.4(3)	N(5)-O(4)-Cu(3)	144.4(5)
O(8)-Cu(1)-N(1)	92.6(3)		

Symmetry transformations used to generate equivalent atoms: #1 -x,y,-z+1/2 ;#2 -x+1, y, -z+ 1/2

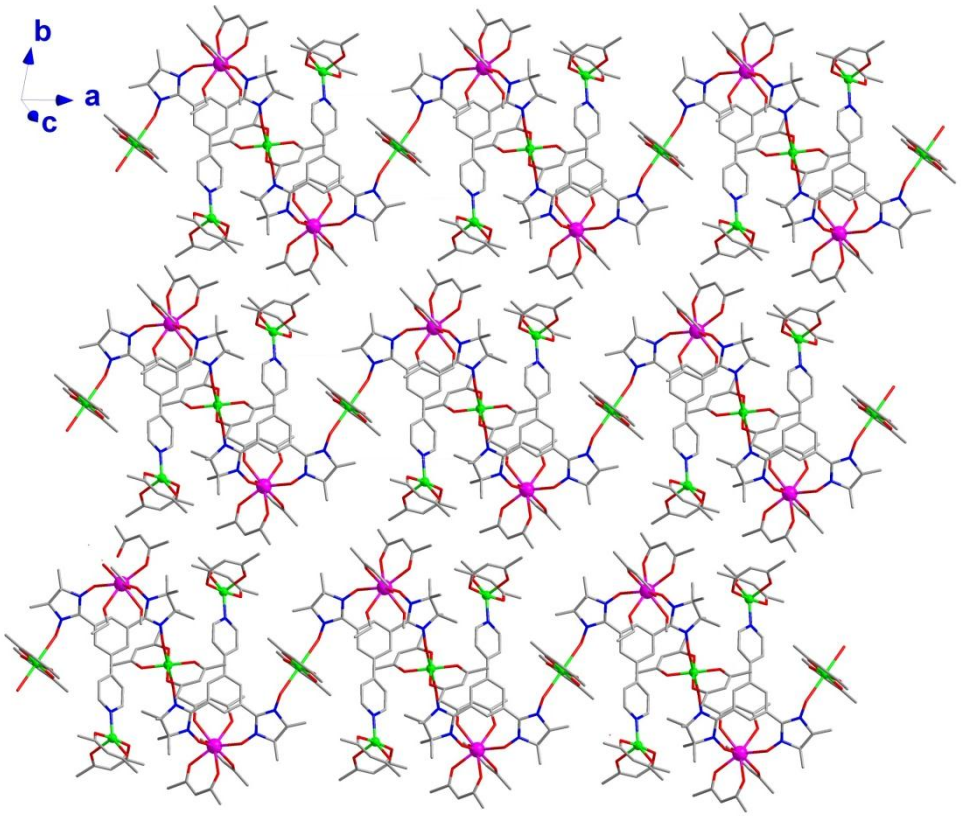

Fig. S1 Packing diagram of complex **1**. All H and F atoms are omitted for clarity.

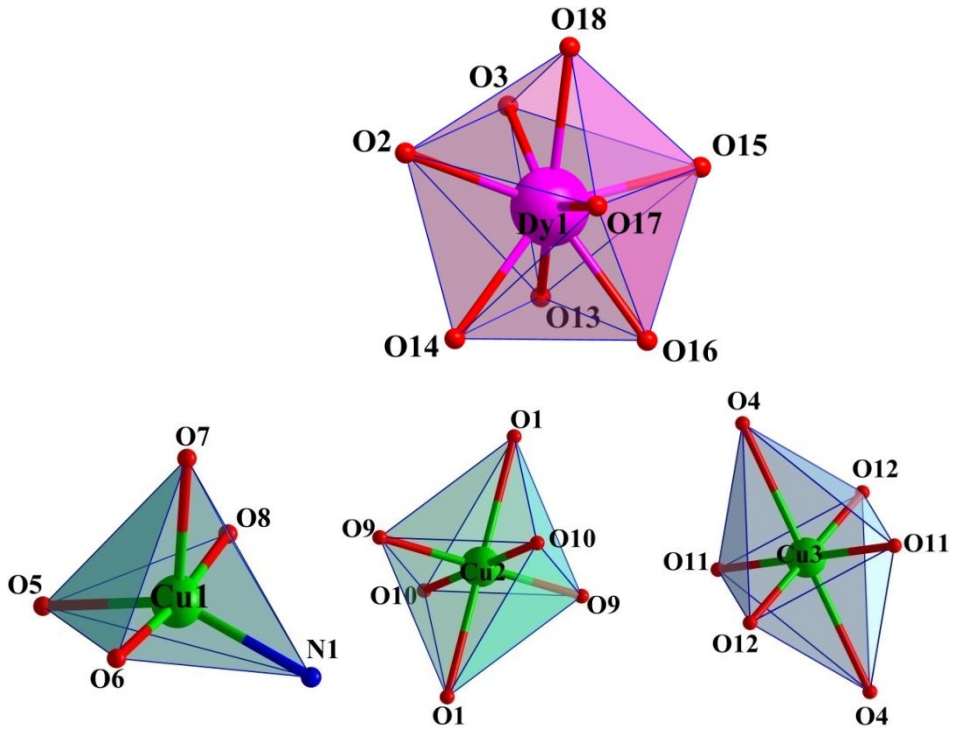

Fig. S2 Coordination polyhedrons of the Dy^{III}, Cu^{II} 1, $Cu^{II}2$ and $Cu^{II}3$ ions.

Table S3 Detailed geometry analysis results by Continuous Shape Measures.

Compound	SAPR-8	TDD-8	JBTPR-8	BTPR-8	JSD-8
1Dy	2.074	1.879	1.489	**0.743**	3.658

SAPR-8: square antiprism. TDD-8: triangular dodecahedron. JBTPR-8 : Biaugmented trigonal prism J50. BTPR-8: biaugmented trigonal prism. JSD-8 : Snub diphenoid J84

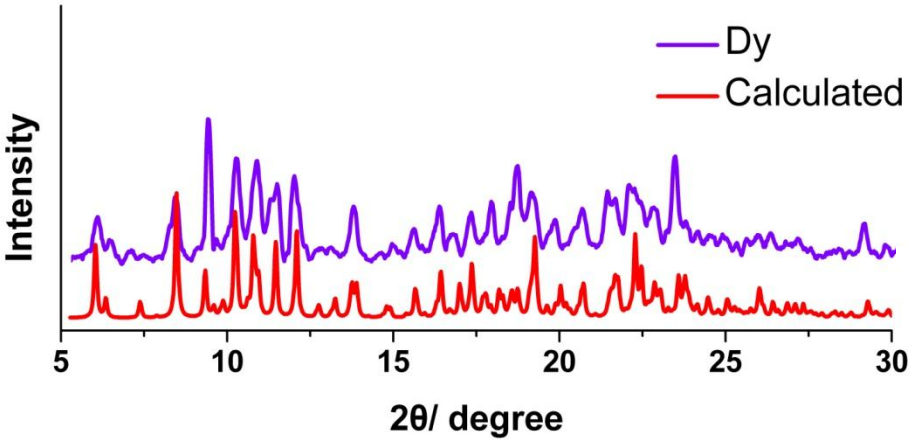

Fig. S3 Powder X-ray diffraction pattern of Dy complex at 293 K, together with the calculated pattern from the crystal structure data.

4. Magnetic measurements

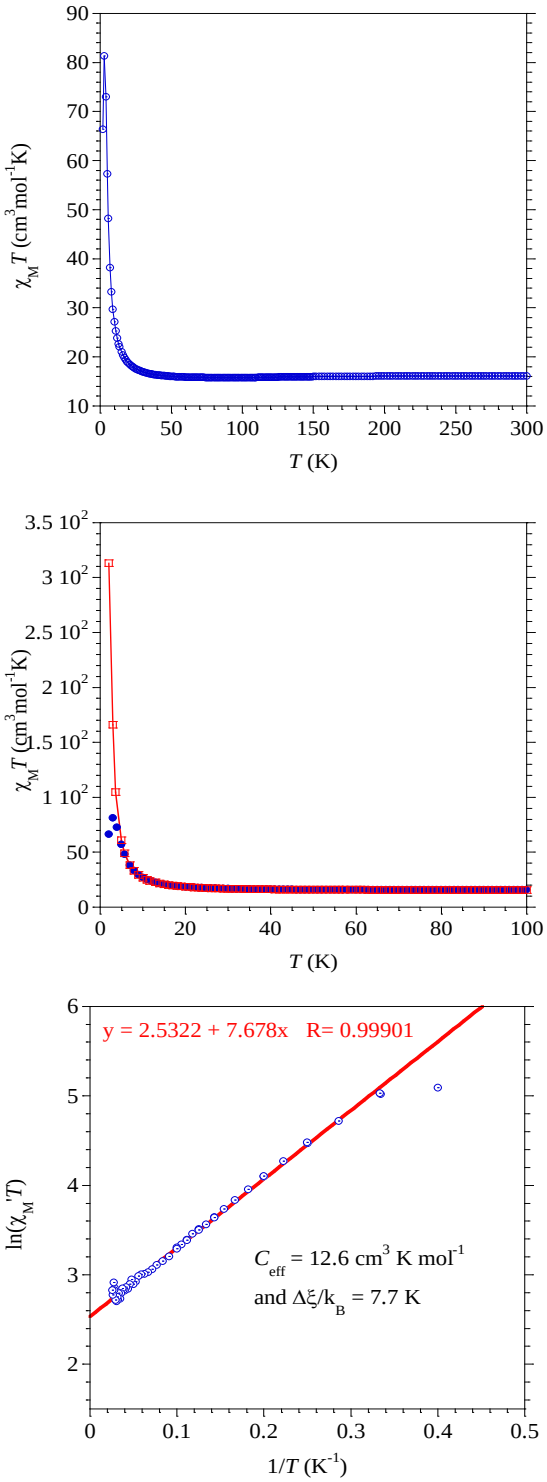

Fig. S4 Temperature dependence of $\chi_M T$ with χ_M (*top*) recorded in an applied field of 1 kOe, *(middle)* variation of $\chi_M T$ below 100 K in an applied field of 50 Oe (in red) and 1 kOe (blue) revealing a saturation effect in larger field; and , *(bottom)* ln(χ_M'T) = f(T^{-1}) (χ_M', the in-phase susceptibility measured with an AC field of 3 Oe (ν = 100 Hz) in the absence of a dc field), the solid red line is the best fit of the Glauber's expression to the linear part between 3 and 25 K.

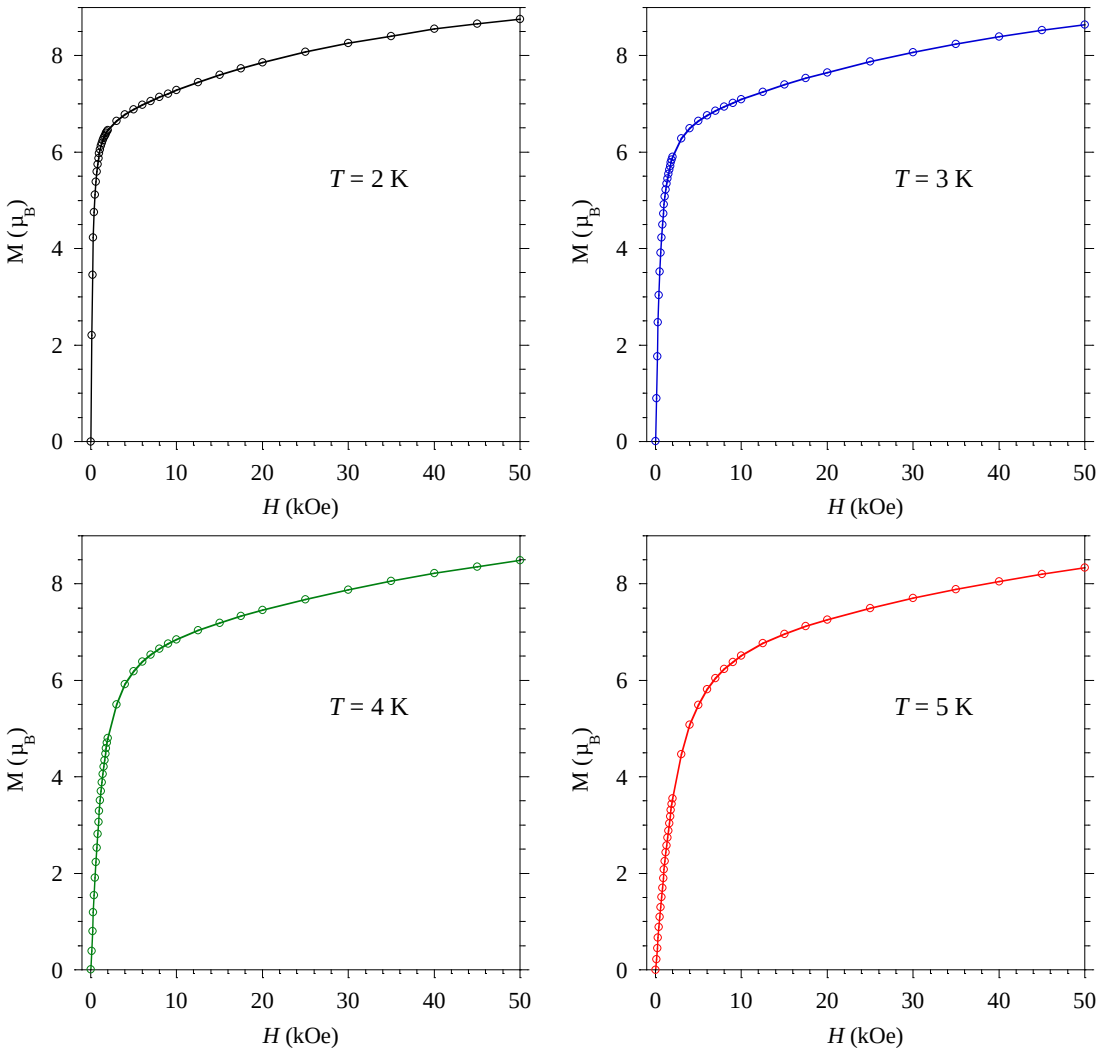

Fig. S5 Field dependence of the magnetization at different temperature for **1**.

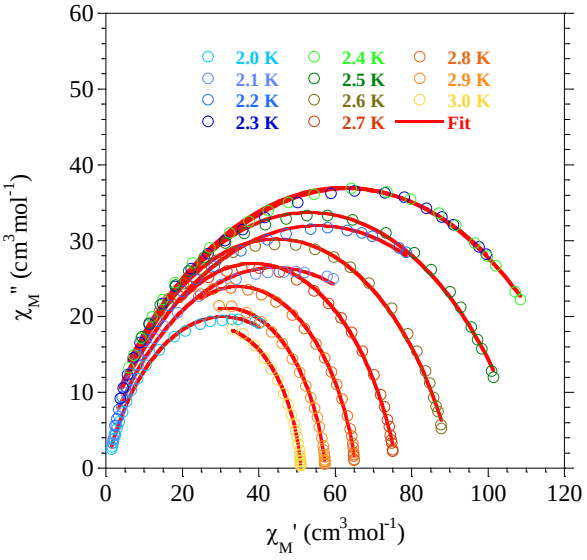

T (K)	χ_{iso}	X_{adia}	α
2.0	61	0.1	0.26
2.1	91	-2	0.34
2.2	115	-4.2	0.37
2.3	131	-4.4	0.36
2.4	130	-5.5	0.36
2.5	111	-4.7	0.32
2.6	91	-2.1	O.27
2.7	76.2	1.1	0.20
2.8	65.5	3.8	0.16
2.9	57.5	5.6	0.13
3.0	51.1	7.2	0.11

Fig. S6 $\chi_M''= f(\chi_M')$, i.e. Cole-Cole plots and best fits (solid lines) with a generalized Debye model, the fit parameters are gathered in the table.

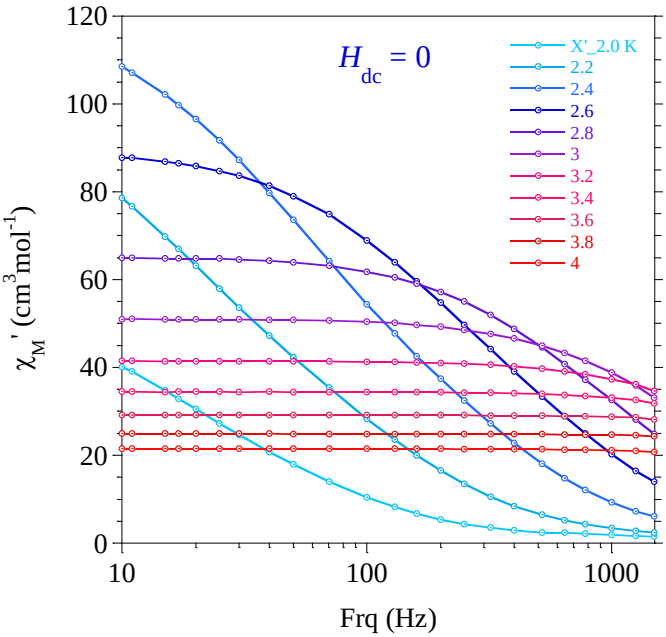

Fig S7. Frequency-dependent in-phase signals (χ') for **1** under zero dc field with H_{AC} = 3 Oe.

5. References

[S1] H. D. Li, J. Sun, M. Yang, Z. Sun, J. K. Tang, Y. Ma and L. C. Li., *Inorg. Chem.*, 2018, **57**, 9757.

[S2] Sheldrick, G. M. SADABS, Program for Absorption Correction of Area Detector Frames, BRUKER AXS Inc., Madison, WI.

[S3] Sheldrick, G. M. SHELXS-2014, Program for structure solution; Universitat Gottingen: Gottingen, Germany, 2014.